applied sciences

MDPI

Article

Electrical Heating of Carbon Textile Reinforced Concrete—Possible Effects on Tensile Load-Bearing Behavior

Annette Dahlhoff * and Michael Raupach

Institute of Building Materials Research (IBAC), RWTH Aachen University, Schinkelstr. 3, 52062 Aachen, Germany
* Correspondence: dahlhoff@ibac.rwth-aachen.de

Abstract: Carbon-textile-reinforced concrete (CTRC) is currently used as a high-performance composite material in the construction industry, comprising concrete and a non-metallic reinforcement. In addition to remarkable material properties such as tensile-load-bearing behavior, durability and density, this innovative material features high electrical conductivity, offering the potential for electrical heat generation within building components. This paper contributes to the field by exploring the unique combination of properties exhibited by carbon-textile reinforcements (CTR) electrically heated up to 80 °C. The impact of the electrical heating of CTR was evaluated by conducting stationary tests on load-bearing behavior. The tests were conducted on two different CTRs: one impregnated with polystyrene, and the other with epoxy resin additionally surface-modified with quartz sand. In order to quantify the influence of individual material parameters, tensile tests were conducted on the components comprising CTR and mortar, as well as the composite CTRC. The analysis focused on electrically heated carbon-textile reinforcements, comparing them through experiments conducted at varying ambient temperatures. This study presents pioneering findings on heated CTRC, determining that electrical heating decreases tensile strength with increasing temperature for the investigated reinforcement materials. The softening of the impregnation materials proved to be a decisive factor. This interdisciplinary approach bridges materials science with thermal management in construction, offering insights into the practical applications of CTR in innovative building designs.

Keywords: carbon textile reinforced concrete; tensile strength test; crack formation; electrical heating; temperature behavior

Citation: Dahlhoff, A.; Raupach, M. Electrical Heating of Carbon Textile Reinforced Concrete—Possible Effects on Tensile Load-Bearing Behavior. *Appl. Sci.* **2024**, *14*, 4430. https://doi.org/10.3390/app14114430

Academic Editor: Ana Martins Amaro

Received: 11 April 2024
Revised: 14 May 2024
Accepted: 21 May 2024
Published: 23 May 2024

1. Introduction

The composite material carbon textile reinforced concrete, referred to as CTRC, is currently being investigated in various sectors of the construction industry to realize resource-efficient construction projects with outstanding materials properties. The composite material CTRC consists of non-metallic reinforcement made of carbon fibers with impregnation with, for example, polymers and concrete. This impregnation activates the inner filaments of carbon for force transmission and adjusts the stiffness of the material. For applications with a demand on bond behavior and crack distribution, fiber strands made of carbon fibers with impregnation are additionally coated with quartz sand and epoxy resin [1]. The low density and chemical resistance of carbon allow for the production of thin, durable and material-minimized building components. Furthermore, this innovative non-metallic building material exhibits tensile strengths of up to 4200 N/mm^2 [2,3].

In this context, the electrical conductivity of carbon fibers, as well as their high thermal conductivity along the fiber direction, can be utilized for the development of electrically heated CTRC. This innovative multifunctional technique can be applied as a heating element in building components using Joule's heating principle [4]. The temperature increase occurs as a result of heating a conductor by applying an electrical voltage. Exemplarily, Figure 1 shows the heating development of various commercially available CTR with various impregnations and current injection points.

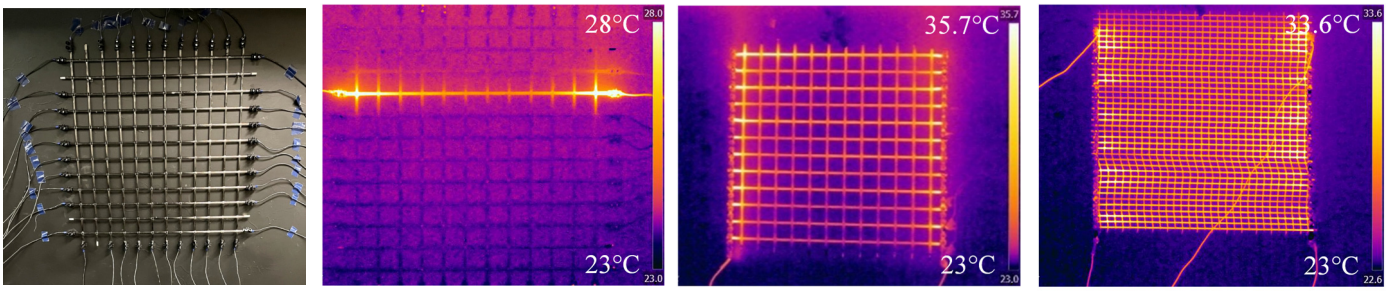

(**a**) (**b**) (**c**) (**d**)

Figure 1. Exemplarily heated CTR: (**a**) connected epoxy resin-impregnated CTR—test setup; (**b**) epoxy resin-impregnated CTR—one fiber strand connected; (**c**) epoxy resin-impregnated CTR—weft fiber strand connected; (**d**) polystyrene-impregnated CTR—weft fiber strand connected.

Nevertheless, to ensure the long-term durability of this heated element, it is imperative to assess its impact on the material properties. This study aims to delve into this aspect, with a particular focus on the tensile-load-bearing behavior of CTRC electrically heated up to 80 °C. For this purpose, the tensile strength and crack distribution characteristics of electrically heated specimens were examined through stationary experimental tests. Stationary tests involve isothermal conditions with constant temperature loading until failure. Of particular significance is the comparison between the results of individual components like mortar as well as carbon fibers with impregnation and composite CTRC. Through laboratory experiments, the influence of electrical heating was quantified and distinguished. Moreover, characteristic values for load-bearing behavior were analyzed. Additionally, experiments were conducted to compare the heating process through electrical heating with ambient temperature conditioning. This facilitates the quantification of whether the development of temperature gradients affects tensile-load-bearing behavior. In contrast to the existing literature, which predominantly focuses on material characteristics under elevated ambient temperatures, this study uniquely investigates the tensile-load-bearing behavior and crack formation of electrically heated CTRC.

In the following, existing studies on the electrical heating function of carbon textile reinforcement (CTR) as well as its applications are summarized, and the temperature behavior of CTRC in ambient conditions based on previous research is characterized.

Electrical heating was investigated using carbon yarns and CTRC specimens by Hasan et al. [5]. Their results indicated that the geometry of CTR impacts electrical conductivity, with resistance increasing with higher filament counts [5]. This phenomenon was further investigated by Gerlach et al. [6], who examined the increase in conductivity with finer yarns. Focusing on thermal prestressing, Schladitz et al. [7] analyzed targeted heating. In this context, electrical contact provides an interface for current input. Investigations of electrical contact were carried out by Hemmen [8], Krois [9], Tröger et al. [4] and Dahlhoff et al. [10]. Furthermore, Dahlhoff et al. examined the influence of geometric changes in specimen dimensions, from 0.25 m^2 to 0.5 m^2, on heat development [10].

Building materials research has investigated the possible application of electrically heated carbon reinforcement through comprehensive studies, innovative concepts and practical implementation in construction projects. Its main application involves integration into building components. For instance, CTR can serve as an electrical resistance heating element, providing capabilities such as radiant heating or heat storage in concrete elements, thereby acting as protection against condensation [11,12]. This was implemented using electrically heated CTRC as a method of radiant heating in wall components [13,14]. In these studies, a hybrid textile reinforcement composed of carbon fibers in the wrap direction and alkali-resistant glass fibers in the weft direction was used [13]. Moreover, the heat generated by the electrically heated CTR had a positive influence on the hydration behavior of the concrete and could be utilized for the de-icing of outdoor facilities, such as car parking spaces or infrastructure [15,16]. Xu et al. conducted numerical and experimental investigations of

the electrothermal properties. In their research, the potential for de-icing through the heat generated in the composite material of carbon/glass fiber hybrid textile-reinforced concrete was validated, as evidenced by both numerical simulations and experimental studies [17].

To implement the proposed application of electrically heated CTRC, investigating the material's behavior under temperature loading is essential. To contextualize the material behavior of electrically heated CTRC and the test results of this study, findings on the components (mortar, carbon fiber and impregnation) as well as the composite are summarized within the investigated temperature range of up to 80 °C [18]. It is noteworthy that these results were obtained through ambient-temperature heating.

Donnini et al. [19] conducted experimental tests to assess the impact of tempering on tensile strength of CTRC. The testing temperatures ranged from 20 to 120 °C, and unimpregnated CTR as well as epoxy resin-impregnated CTR with additional sanding were used. The unimpregnated material showed no strength loss due to temperature exposure, whereas the epoxy resin-impregnated material exhibited a reduction of up to 70% when tested at 80 °C. These results, as shown in Figure 2, led to more pronounced reduction compared to other findings. Consequently, reductions of this magnitude are not expected for CTRC. Furthermore, the structural functionality of the epoxy resin-impregnated material was preserved after exposure to high temperatures and subsequent cooling [19]. Additional expansion tests up to 80 °C with epoxy resin-impregnated CTR with additional sanding were conducted by Morales [1]. A reduction in tensile strength of up to 4.4% at 80 °C in comparison to 23 °C was highlighted. An increase in testing temperature corresponded to a lower number of cracks alongside an increase in the average crack width [1]. In comparison, Rambo et al. conducted tensile tests on CTRC, specifically basalt fibers impregnated with styrol-acrylate in conjunction with refractory concrete [20,21]. These tests were conducted at elevated temperatures ranging from 75 to 1000 °C, as well as after preheating and testing at room temperature. The results demonstrated an increase in tensile strength of 43% for specimens heated up to 150 °C. In addition, a finer crack pattern with increasing test temperature was observed with digital image correlation (DIC) [20]. Lenting [22] examined the temperature behavior of silicic acid ester-impregnated reinforcement, ranging from 80 to 160 °C. The results indicated a reduction in average crack width with increasing temperature, while the tensile strength was not negatively affected up to 160 °C [22]. The results from the literature on the elevated-temperature behavior of the reduction factor K_T in relation to tensile strength at a specific temperature of 20 °C for ambient heating are summarized in Figure 2.

$$K_T = F_T/F_{20°C}, \quad (1)$$

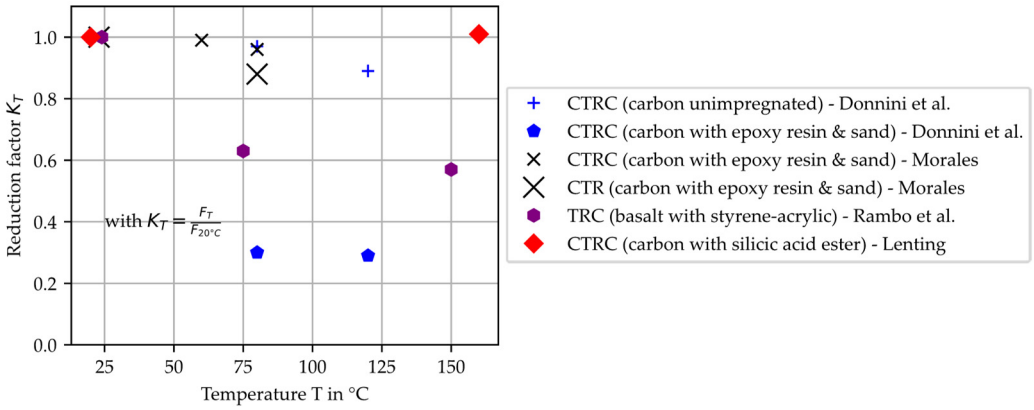

Figure 2. Results from the literature on behavior in temperatures elevated up to 160 °C for the reduction factor K_T in relation to tensile strength at a specific temperature of 20 °C [1,18–20,22,23].

The components of the above equation are defined as follows:
K_T is the reduction factor;
F_T is the tensile strength at a specific temperature in N/mm^2;

$F_{20°C}$ is the tensile strength at a temperature of 20 °C in N/mm^2.

In order to characterize the potential of electrically heated CTR in construction materials, particularly focusing on their behavior and performance under varying thermal conditions, experimental tests were conducted using CTRC uniaxial tensile specimens. Contrasting with the existing literature, which primarily discusses material characteristics under elevated ambient temperatures, this paper uniquely examined the tensile-load-bearing behavior and crack formation of electrically heated CTRC.

2. Materials

In this study, two carbon textile reinforced composites composed of a commercially available CTR and a repair mortar, according to [24,25], were used for the evaluation. The investigated CTR are characterized by different material properties, determined by the varying impregnation materials. One carbon textile impregnated with epoxy resin and additionally surface-modified, referred to as CTR-EP-Sand, with a rectangular roving axis distance of 21 mm and an equal roving cross-section of 0.90 mm^2 in the wrap and weft directions was used. The surface modification involved a subsequent coating of epoxy resin and quartz sand. In addition, a carbon textile impregnated with polystyrene, referred to as CTR-P, with a roving axis distance of 12/16 mm and an equal roving cross-section of 1.81 mm^2 in the wrap and weft directions was used. The investigated carbon-textile reinforcements are shown in Figure 3, and the material parameters are summarized in Table 1.

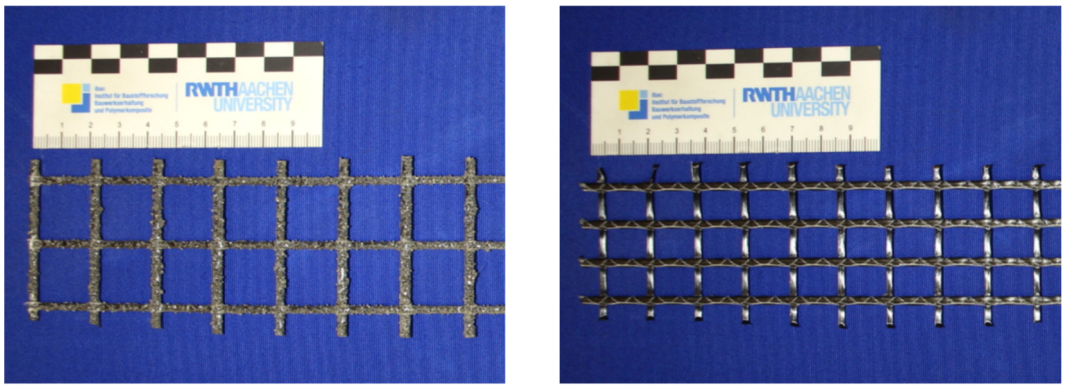

(**a**) (**b**)

Figure 3. Investigated carbon textile reinforcements: (**a**) CTR-EP-Sand; (**b**) CTR-P.

Table 1. Material parameters of the carbon textile reinforcement according to the manufacturer's specification [26].

Reinforcement	Roving Axis Distance	Roving Cross-Section	Textile Cross-Section	Titer	Average Tensile Strength (Wrap Direction)	Average Ultimate Strain (Wrap Direction)
	Longitudinal/Transversal					
[-]	[mm]	[mm^2]	[mm^2/m]	[Tex]	[MPa]	[‰]
CTR-EP-Sand	21/21	0.90/0.90	43/43	1600/1600	4200 ± 215 [1]	15 ± 1.5 [1]
CTR-P	12/16	1.81/0.45	142/25	3220/800	2920 ± 95 [1]	13.5 ± 2.7 [1]

[1] Measurements performed at the Institute of Building Materials Research (IBAC), RWTH Aachen University, Aachen, Germany.

For the investigations of the composite, a polymer-modified cement-based mortar designed for repairing and retrofitting concrete surfaces, with a maximum grain size of 2 mm, was used according to TR IH [24,25]. The material properties of the mortar are shown in Table 2.

Table 2. Material parameters of the repair mortar.

Mortar	Compressive Strength [1]	Bending Strength [1]
[−]	[MPa]	[MPa]
SRM-A4	72 ± 3	4 ± 0.5

[1] Measurements performed at the Institute of Building Materials Research (IBAC), RWTH Aachen University.

3. Experimental Methods

3.1. Methods

To investigate the impact of electrical heating on the presented textile reinforcement materials, stationary tensile strength tests were performed on both the individual components and the composites. For this, tensile strength tests on briquet mortar specimens according to ASTM C307-18 [27] were conducted in a climatic chamber within a temperature range of 20 to 80 °C. Through the utilization of the climatic chamber, samples could be subjected to controlled heating through ambient air, facilitating testing at specific temperature stages. This heating method is referred to as AH for ambient heating. In addition to individual tests on SRM-A4, uniaxial tensile strength tests were carried out on the CTR at specific temperatures of 20 to 80 °C. Within this temperature range, the operational temperature range of the heating function could be investigated, establishing limited temperature ranges. The CTR was electrically heated (EH), and for comparative temperature analysis, the CTR was exposed to ambient temperature (AH) within a climatic chamber. The results of uniaxial fiber strand tensile strength tests on CTR-EP-Sand are compared with the results from [10].

In comparison to the laboratory experiments of the individual components, the mortar and fiber strand, uniaxial tensile strength tests were conducted on the composite CTRC. The material combinations were exposed to temperature variations ranging from 20 to 80 °C. Both electrical (EH) and ambient (AH) heating processes were conducted on the CTRC composite, and the results were compared with each other. Table 3 gives an overview of the investigated experimental test series.

Table 3. Overview of the investigated experimental test series.

Experimental Tests		Number of Test Specimens per Temperature Level	Testing Temperature in Laboratory Experiments		
			CTR-EP-Sand	CTR-P	SRM-A4
		[-]	[°C]		
Tensile strength test according to ASTM C307-18	AH [3]	4	-	-	20/40/60/80
Uniaxial fiber strand tensile strength tests on CTR	AH	4	20/40/60/80	20/40/60/80	-
	EH [4]		20/40/60/80	20/40/60/80	-
Uniaxial tensile strength tests on CTRC uniaxial tensile specimens [1]	AH	3	20/40/60/70 [2]	20/40/60/70	-
	EH		20/40/60/70	20/40/60/70	-

[1] Respective carbon textile reinforcement in combination with SRM-A4. [2] Testing temperatures between 70 to 80 °C. [3] Ambient heating = AH. [4] Electrical heating = EH.

3.2. Experimental Setup and Testing Procedure

The experimental setup and testing procedure are subdivided into three sections. Initially, tensile strength tests on the individual components, mortar and CTR, are presented, followed by the subsequent CTRC experiments.

3.2.1. Tensile Strength Tests on Briquet Mortar Specimens

The tensile strength tests on SRM-A4 were carried out on briquet specimens according to ASTM C307-18 [27] with the experimental setup based on Dahlhoff et al. [28], depicted in Figure 4.

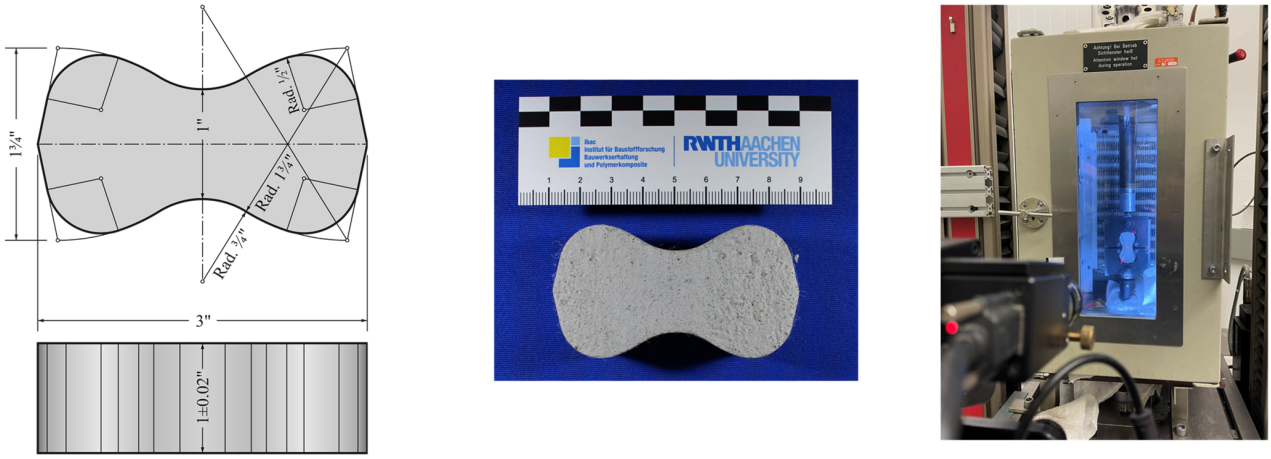

(**a**) (**b**) (**c**)

Figure 4. Tensile strength test setup adapted from [27,28]: (**a**) technical drawing of briquet specimen; (**b**) briquet specimen SRM-A4; (**c**) test setup in climatic chamber.

The SRM-A4 was mixed in a ratio of solid to water weight content of 1:0.13. Subsequently, the fresh-mortar properties were determined according to [29] (consistence), [30] (bulk density) and [31] (air content). Standard prism sets were prepared to determine the flexural and compressive strengths for the respective test dates of the tensile tests in accordance with [32]. The specimens were stripped of the formwork after one day and stored in water for 24 days. Afterwards, the specimens were stored in a climate-controlled room at a temperature of 22 °C and a relative humidity of 53% until testing at the age of 28 days. For each temperature level, four samples were examined [28].

For testing, the specimens were pulled centrically using clamps installed in the climatic chamber type TEE 26/LN2 with JULABO CF 41, using a 150 kN universal testing machine Zwick Z150 TL. A preload of 200 N was applied and a displacement control rate of 0.6 mm/min was maintained until specimens' failure occurred. The load, crosshead displacement and temperature of the climatic chamber were recorded in the software TestXpert® Version 3.6. Before testing, the specimens were preheated in the climatic chamber for 20 min to achieve uniform temperature, with the surface temperature monitored using an Flir E96 thermal imaging camera.

3.2.2. Tensile Strength Tests on CTR

To investigate the influence of temperature development on tensile strength, tensile tests were conducted on commercially available fiber strands (FS). Since commercially available FS were used, a separate examination of the impregnation materials and coating was not conducted. For the tensile strength tests, FS in the wrap direction with a total length of 500 mm were cut out from the textile reinforcement grid and cast into 150 mm long steel hulls using grout mortar. The FS made of CTR-P were additionally coated at the ends using a two-component structural adhesive composed of epoxy resin and quartz sand [10]. For the experiments with electrical heating, the ends of the FS were connected using ferrules and terminal strips, and then linked to a laboratory power supply. The target temperature levels were set by adjusting the voltage, and the temperature of the FS surface at the 200 mm free testing length was measured using the Flir E96 thermal imaging camera. Table 4 provides an overview of the electrical parameters used to set the target temperatures.

Upon reaching the target temperature, uniaxial tensile tests were conducted in a Zwick Z150 TL 150 kN universal testing machine, maintaining a controlled testing speed of 2 mm/min, as shown in Figure 5. The load, crosshead displacement and temperature of the climatic chamber were recorded in the software TestXpert®. In the test series, deformation was recorded using two extensometers with a gauge length of 100 mm, and the strain was calculated accordingly. The strain at specimen failure was examined based on the

linear-elastic material behavior of CTR through linear regression on the stress–strain curve, using the determined tensile strength [1,22,33].

Table 4. Mean electrical parameters for heating the FS tensile specimens [10].

Target Temperature	CTR-EP-Sand		CTR-P	
	Terminal Voltage	Current	Terminal Voltage	Current
[°C]	[V]	[A]	[V]	[A]
40	7	0.4	3.9	0.7
60	17.5	0.7	5.5	1.1
80	16.7	0.9	3.7	1.2

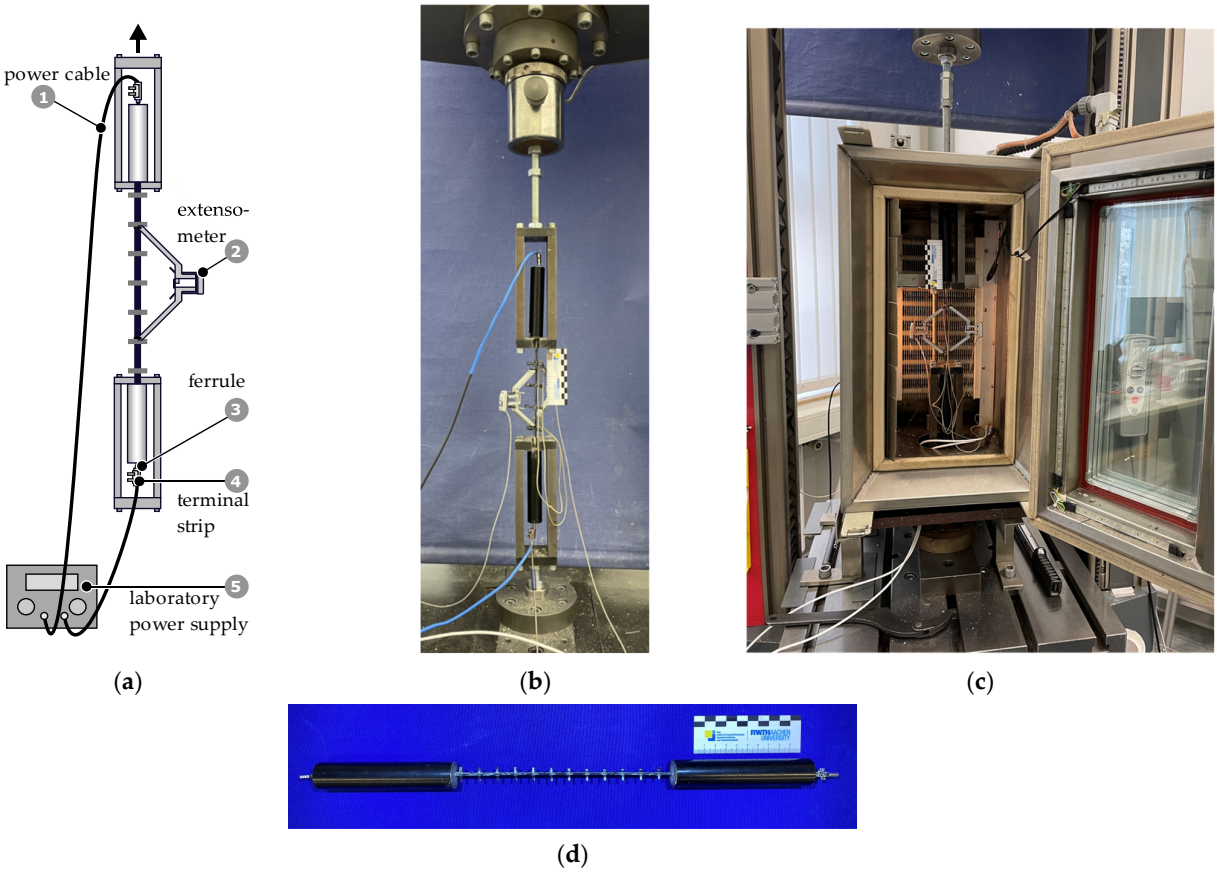

Figure 5. FS tensile strength test setup: (**a**) schematic drawing; (**b**) overview of EH test setup; (**c**) overview of AH test setup; (**d**) exemplary fiber strand CTR-P.

Comparative investigations were carried out using an identical test setup in a TEE 26/LN2 climatic chamber with JULABO CF 41, as depicted in Figure 5, following a 20 min conditioning period of the FS. Five specimens were examined in each batch.

3.2.3. Tensile Strength Tests on CTRC

To determine the tensile behavior of CTRC under electrical and ambient heating, tensile strength tests were conducted on rectangular CTRC specimens, depicted in Figure 6. The specimen dimensions were 500 × 60 × 20 mm^3 (L × W × T), both produced with a constant mortar cover using SRM-A4 on both sides and a single layer of CTR. The specimens were hand-laminated using a ratio of solid to water weight content of 1:0.13. Subsequently, the fresh-mortar properties were determined according to [29–31] and standard prism sets were prepared to determine the flexural and compressive strengths for the respective test dates of the tensile tests in accordance with [32].

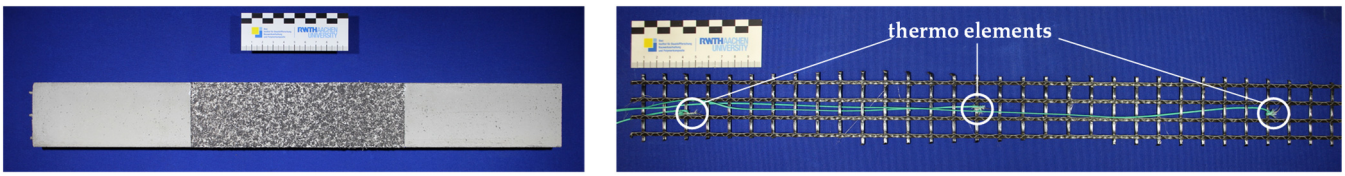

(**a**) (**b**)

Figure 6. CTRC uniaxial tensile specimens: (**a**) exemplary CTRC-EP-Sand specimen; (**b**) positionof thermal elements on the CTR exemplarily CTR-P.

For the electrical heating experiments, the ends of the specimens were connected using ferrules and terminal strips, and then linked to a laboratory power supply. The target temperature levels were set by adjusting the voltage. Comparative investigations were carried out using an identical test setup in a TEE 26/LN2 climatic chamber with JULABO CF 41. The temperature was observed using the Flir E96 thermal imaging camera on the surface of the CTRC uniaxial tensile specimen and additional thermo elements directly on the grid, as depicted in Figure 6. In each batch, the core temperature development was analyzed using thermal elements in the initial test, subsequently leading to the determination of the heating period's duration. The thermal elements were positioned relative to the lower edge at 20 mm, 250 mm and 480 mm. The surface temperature was checked before each test using a thermal imaging camera, and if the target temperature was not achieved, the heating period was extended. Table 5 provides an overview of the electrical parameters used to set the target temperatures and the duration for the conditioning period within the climatic chamber based on the thermal camera and core temperature.

Table 5. Mean electrical parameters for heating the CTRC tensile specimens.

Target Temperature	CTR-EP-Sand				CTR-P			
	EH			AH	EH			AH
	Terminal Voltage	Current	Duration	Duration	Terminal Voltage	Current	Duration	Duration
[°C]	[V]	[A]	[min]	[min]	[V]	[A]	[min]	[min]
40	16	3.5	15	30	7	6	15	30
60	17	4	60	30	9	7	60	30
70	17	4	140	90 [1]	11	7	120	45

[1] Testing temperature between 70 and 80 °C.

For testing, the rectangular specimens were clamped in steel plates in the upper and lower load introduction areas over a length of 150 mm, cf. Figure 7. A torque of 25 Nm was applied. The tensile strength tests were carried out using a Zwick Z150 TL 150 kN universal testing machine, maintaining a displacement control rate of 2 mm/min until specimen failure. The load, crosshead displacement and temperature of the climatic chamber as well as the core temperature were recorded in the software TestXpert®.

To analyze the full-field deformation of the surface during the tests, the contact-free optical 2D/3D-measuring system ARAMIS® from GOM GmbH was simultaneously used. This system determined the exact load- and time-dependent measurements of crack formation and development. Therefore, a stochastic pattern was applied on the measuring area of CTRC uniaxial tensile specimens. With 5M pixel cameras, the measurement system was calibrated with a measuring volume of 210 × 180 × 175 mm^3, a mean calibration deviation of 0.099 pixel and a scale deviation of 0.001 pixels. For the deformation analysis, 5 images per second were taken. Based on the results from [34], the facet size was set to 15 × 15 pixels and the pixel overlap to 3 pixels, and the threshold for major strain was defined as 0.5%.

For the evaluation of the CTRC specimens, an automated crack evaluation tool (ACE) based on [34] was used. This tool automates the determination of crack width, crack

number, and crack distribution. Additionally, virtual extensometers can be added for strain analysis. In the analysis, the *x*-axis was defined along the tensile direction, with the *y*-axis oriented perpendicular to it.

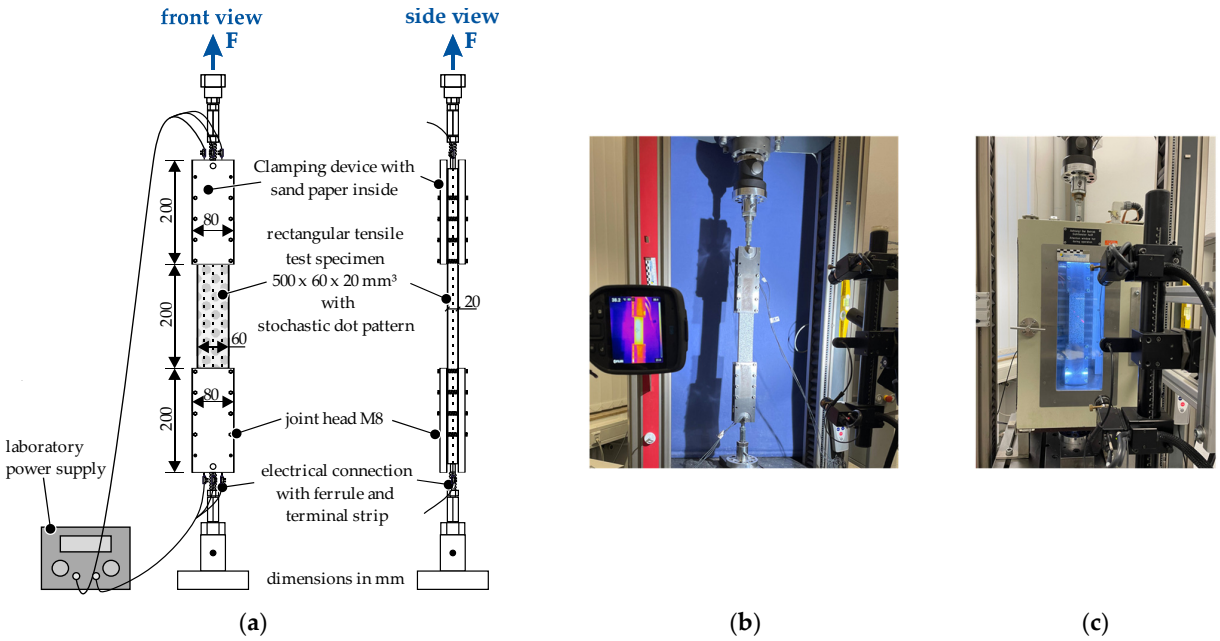

Figure 7. Test setup for the tensile strength tests on rectangular CTRC specimens: (**a**) schematic drawing; (**b**) overview of EH test setup; (**c**) overview of AH test setup.

4. Results and Discussion

4.1. Experimental Results of the Individual Components

4.1.1. Experimental Results of CTR

Initially, tensile strength tests were conducted at a reference temperature of 20 °C. All test specimens failed at the 200 mm free testing length. On average, the CTR-EP-Sand exhibited nearly 1.3 times higher tensile strength values compared to CTR-P, cf. Figure 8a. Therefore, this analysis highlights the impact of impregnation material and geometry on tensile strength. Additionally, as acknowledged in [1], the composite within the fiber strand consisting of impregnation and carbon fiber, as well as manufacturing quality, are decisive factors for strength reduction.

For the data analysis, the reduction factor K_T at each investigated temperature level was determined relative to the tensile strength at a testing temperature of 20 °C, as depicted in Figure 8b. As expected from literature, the results of the fiber strand tensile tests indicated a decrease in tensile strength up to 20% with increasing test temperature [1,19]. In comparison to the reference experiments at 20 °C, the materials CTR-EP-Sand and CTR-P, heated with EH, decreased in average tensile strength by up to 10%. The polystyrene-impregnated material CTR-P with AH showed a decrease of up to 23%, cf. Figure 8b. Exceeding the glass transition temperature T_g of polystyrene of approx. T_g = 100 °C [35,36] can result in a rapid stiffness decrease, leading to softening of the coating and impregnation material and, thus, reduced tensile strength [1]. It should be noted that softening occurs within a temperature range; hence, the process can initiate as early as 80 °C. The decrease in the strength of CTR-P (AH) can thus be attributed to softening of the impregnation. Furthermore, due to the testing methodology, the energy input was prolonged with AH, allowing the softening and thus the chemical reaction to persist for an extended duration prior to testing. To ensure the core temperature, the test specimens were tempered for 20 min. In contrast, the heating of CTR-P with EH was notably accelerated, as the current flow directly adjusts the core fiber strand temperature. Within 3 min, the surface temperature could be reached, verified using the thermal imaging camera.

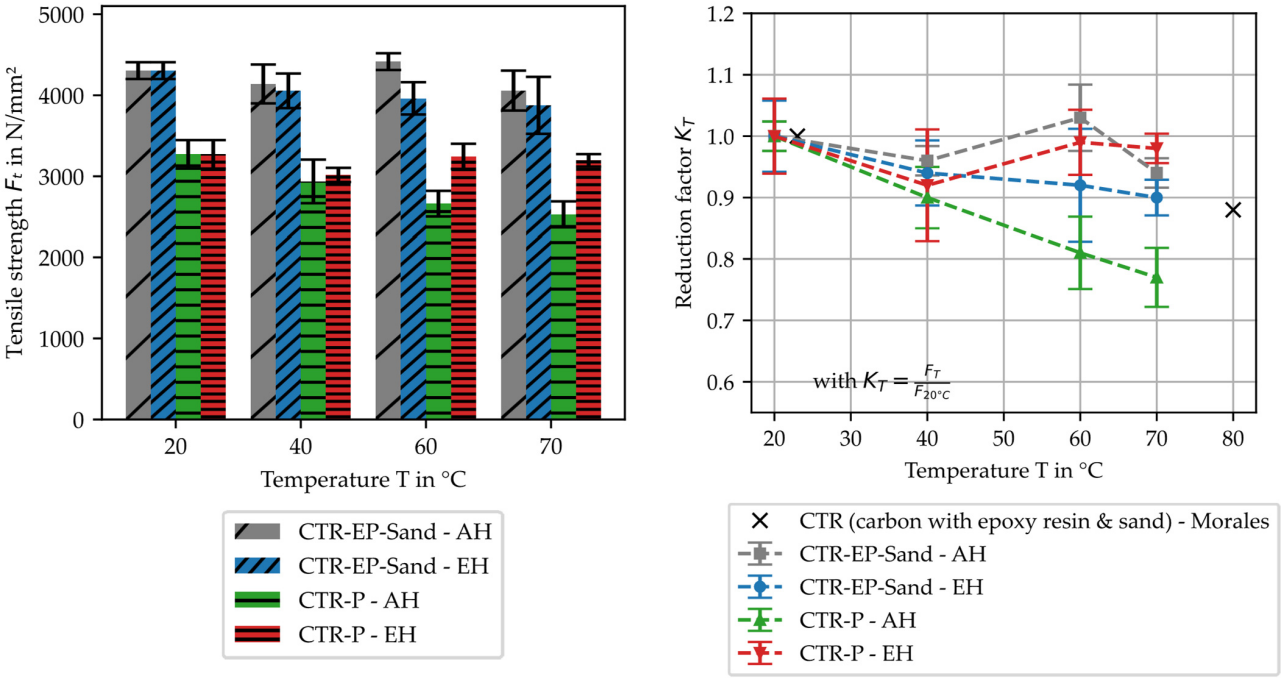

Figure 8. Stationary fiber strand tensile strength test: (**a**) mean values of the tensile strength adapted from [10]; (**b**) reduction factor K_T shown as mean values of tensile strength with standard deviation [1].

In comparison with the CTR, the strain of CTR-EP-Sand was 1.2 times higher than CTR-P at the reference temperature of 20 °C, cf. Figure 9. As the testing temperature increased, no significant deviations from the reference results were observed for the examined materials. However, comparing AH and EH, an increase in mean ultimate strain of up to 13% was examined for EH. The authors assume that direct heat generation in the filament caused it to expand more.

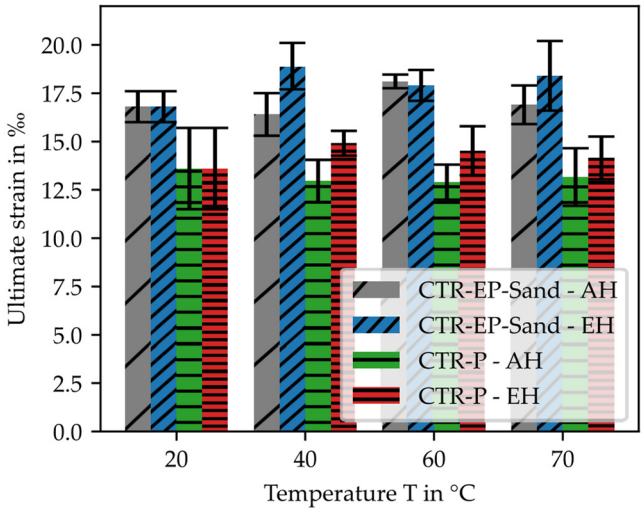

Figure 9. Mean values of ultimate strain of CTR with standard deviation at increasing testing temperatures.

4.1.2. Experimental Results of Repair Mortar

To investigate the tensile strength of repair mortar, the results of the tensile strength tests on the briquet specimens at increasing temperatures (presented as mean value with standard deviation) are summarized in Figure 10. The tensile strength of the investigated mortar decreased by 15% with increasing temperature levels compared to 20 °C. The results

at 40 °C exhibited a significant reduction; however, this can be attributed to test outliers, considering a variation coefficient of 13%. The authors assume that the decrease in tensile strength of mortar can be attributed to mass loss due to evaporation. However, these results can be consistently aligned with the literature findings. According to the results in [37,38], higher strength reduction is known to occur in the tensile zone compared to the compressive zone under elevated temperature conditions. Furthermore, our experimental test results are consistent with the reduction factors identified by [39]. In order to consider creep phenomena, transient tests with constant load levels and increasing heating rates until failure should be investigated.

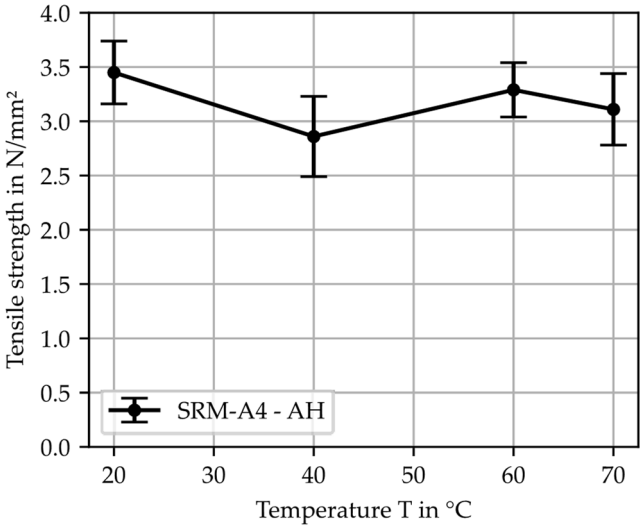

Figure 10. Mean values of the tensile strength with standard deviation of SRM-A4 at increasing testing temperatures.

4.2. Experimental Results of CTRC

To evaluate the load-bearing behavior of CTRC, initially, the tensile strength F_T and reduction factor K_T of the CTRC uniaxial tensile specimens was analyzed. For CTRC-EP-Sand, no influence of tempering was observed on the tensile strength with increasing test temperature. The tensile strength decreased up to 2% at 40 °C and 5% at 70 °C compared to room temperature, cf. Figure 11. However, for CTRC-P, tempering with AH led to a 23% decrease in tensile strength. As hypothesized in Section 4.1.1, this might be attributed to the softening of the impregnation. The comparison of the experimental findings with the literature reveals that the reduction factors correspond to the AH test results reported by [1,20]. Conversely, the results from [19] exhibit substantial deviations. The investigated material combinations indicated a decrease in tensile strength with increasing testing temperature and no adverse effects on the tensile strength of CTRC due to the electrical heating process.

Additionally, the influence of the SRM-A4 layer on the CTR can be examined in the comparison between the tensile strength results of the CTR, cf. Figure 8 (Section 4.1.1), and CTRC, cf. Figure 12. A partly higher tensile strength is achieved in the CTR tests than in the CTRC uniaxial tensile specimens. This elevated strength is observed for both the EH and AH processes. The ratio of CTRC's tensile strength to that of CTR, based on the averages, is at a minimum of 96% at 20 °C for CTRC-EP-Sand. In comparison, the ratio for CTRC-P is lower, with a minimum value of 86% at 20 °C. The authors assume that the increased textile strength can be attributed to mechanical bonding effects. Additional coating with sand enhances the bond to the mortar. In the tensile testing of CTRC-EP-Sand, the mechanical behavior of the fiber strand is not affected, whereas in CTRC-P, the additional coating is absent and local mechanical effects can occur. Furthermore, as explained by [1,40], higher textile strength can be ascribed to the distribution of force applied through transverse

pressure on multiple fiber strands of the CTR, unlike single roving, resulting in more uniform load distribution. Additionally, the method of testing can also impact the results. Firstly, the fiber strand tensile test is conducted without transverse pressure. Secondly, an imprecise alignment of CTRC in the clamping mechanism may induce multi-axial loads and consequently lead to decreased tensile strength.

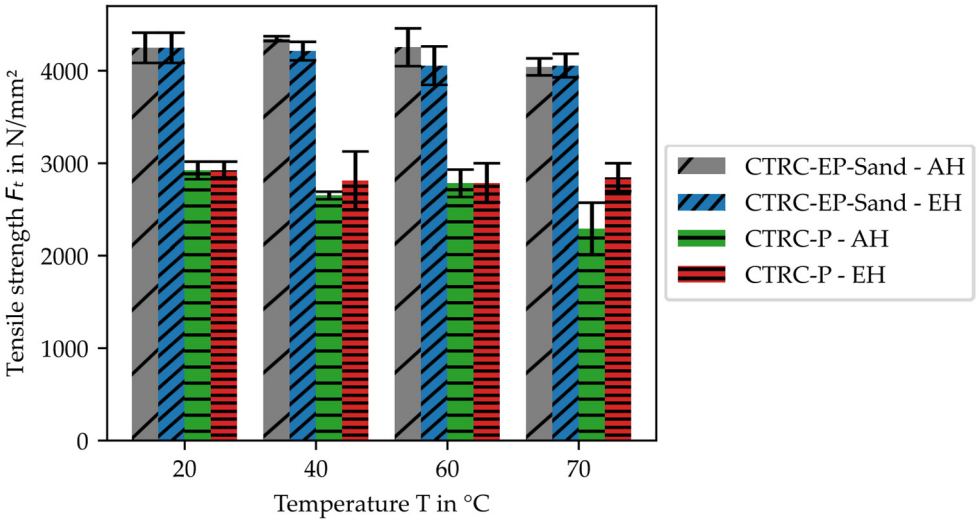

Figure 11. Mean values of the tensile strength of CTRC uniaxial tensile specimen for EH and AH with standard deviation.

When comparing the strain at failure, there was no variation for CTRC-EP-Sand heated with AH, cf. Figure 13. However, the results from the EH test series indicated a decrease in strain with increasing test temperature by 12% compared to 20 °C. For CTRC-P, the strain did not exhibit a clear trend with increasing test temperature and demonstrated a high standard deviation. Regarding the investigation of the influence of EH, the results were not consistent for the two examined materials. Consequently, a uniform conclusion cannot be reached; nevertheless, it is noteworthy that the effect of EH on strain is not typical.

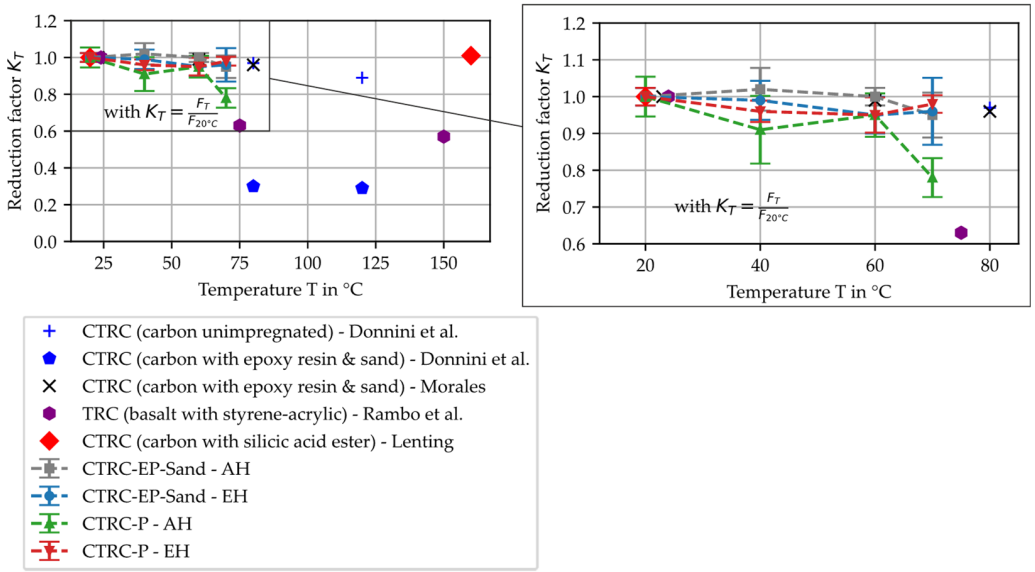

Figure 12. Reduction factor K_T shown as mean values of tensile strength with standard deviation for CTRC [1,19,20,22,23].

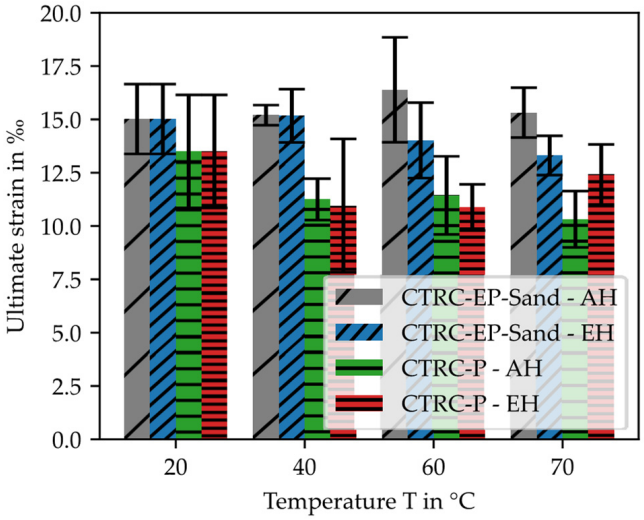

Figure 13. Mean values of the ultimate strain of CTRC with standard deviation at increasing testing temperatures.

With the assistance of DIC measurements and the evaluation tool ACE, crack width and crack distribution were analyzed. Figure 14 demonstrates the relationship between tensile strength and crack width opening in correlation to strain for an exemplary CTRC specimen. The lines in blue depict the width of an individual crack within the specimen. Three distinct stages can be identified: the uncracked stage, crack development and the final crack pattern. These results align with the description of stages provided in the literature on the material behavior of CTRC [1,41–43]. Regarding the material behavior of the electrically heated specimens, the crack development stage was thus not adversely affected by the electrical current flow. The stress–strain curves depicted in Figure 14 are provided as examples and correspond to the trends observed in the subsequent experiments.

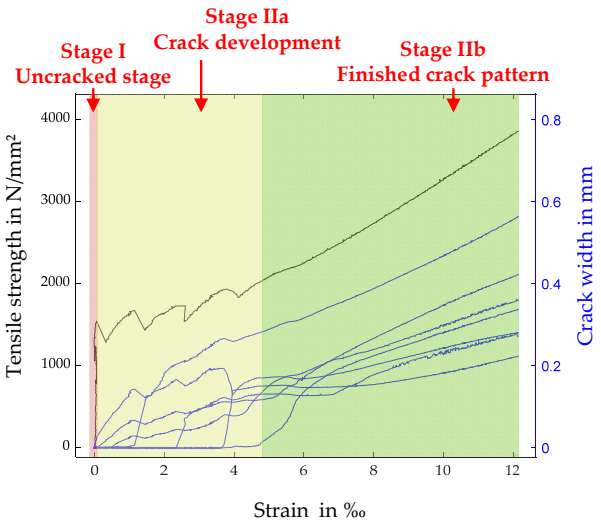

Figure 14. Representative stress–strain curves for uniaxial tensile loading with crack width opening of CTR-EP-Sand.

For the crack analysis, the number of cracks at failure and their respective average crack widths for each test temperature were examined. The results showed that CTRC-EP-Sand exhibits more and smaller cracks compared to CTRC-P. This suggests positive bonding behavior of CTR-EP-Sand, correlated with its higher tensile strength. As discussed, this can be ascribed to the additional sanding of the CTR. With increasing temperature, a decrease from nine to seven cracks was observed for CTRC-EP-Sand in AH. In contrast,

this tendency was less pronounced for CTRC-P, reducing from five to four cracks. The overall reduced crack formation at higher temperatures, compared to 20 °C, is attributed to the softening of the coating and impregnation material of CTR, resulting in reduced bond behavior [1,44].

Additionally, it is noticeable that for CTRC-EP-Sand, electrical heating increased the number of cracks compared to AH, as seen in Figure 15, while reducing the average crack width. Therefore, the authors assume that EH has a positive effect on crack distribution by promoting the occurrence of numerous small cracks. However, this effect is more pronounced in CTRC-EP-Sand. The authors assume that the flow of the electric current induces post-curing of the epoxy resin impregnation material. In a thermosetting plastic, re-crosslinking is an inherent possibility, which could enhance bond behavior and explain the positive effect on the number of cracks. Conversely, for polystyrene, an amorphous thermoplastic, this phenomenon cannot occur.

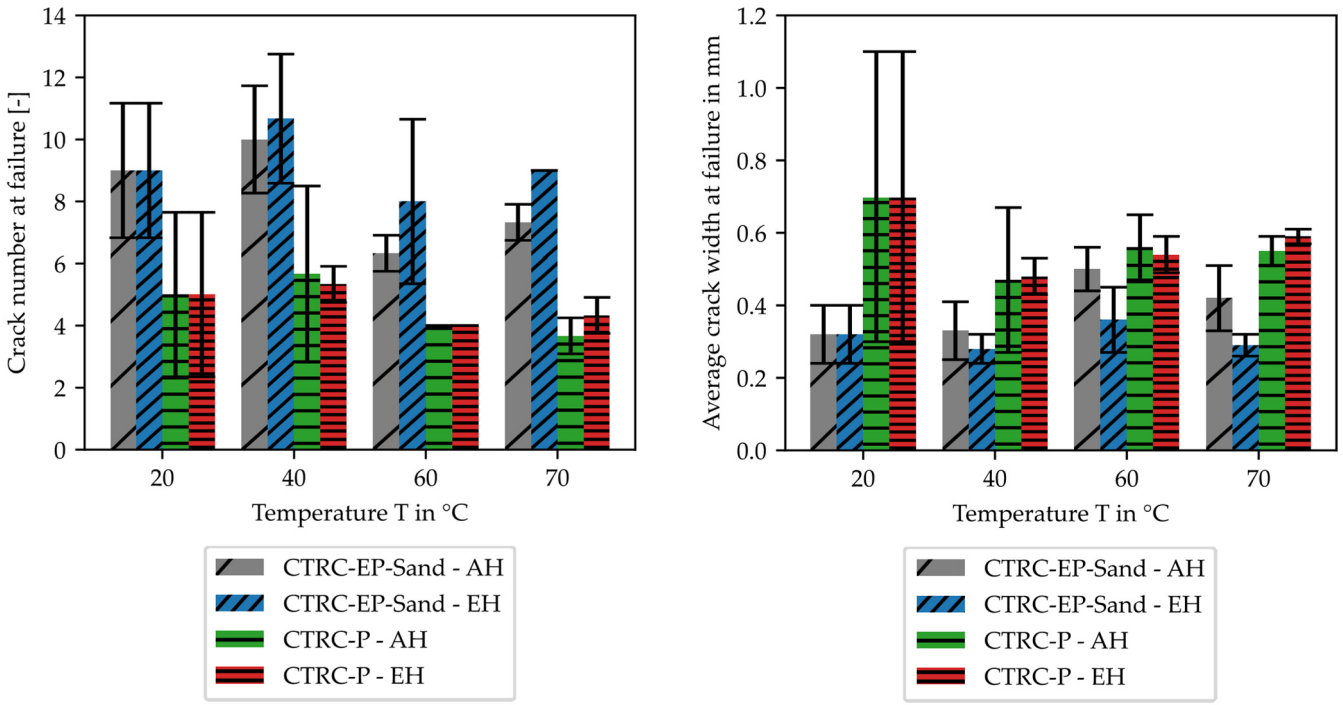

(**a**) (**b**)

Figure 15. Crack analysis of CTRC—mean values with standard deviation: (**a**) number of cracks at failure; (**b**) average crack width at failure.

For further investigation, Figure 16 shows representative crack patterns immediately before failure for the CTRC uniaxial tensile specimens sorted by EH and AH at rising test temperatures. Additionally, the weft fiber strands are shown schematically. The increased number of cracks for CTR-EP-Sand is depicted in Figure 16. However, no influence on the crack pattern, such as an irregular width across the entire cross-section or a bulging trajectory, can be observed with EH. Therefore, in the event of a crack occurring in the composite structure and being influenced by electrical heating, it can be assumed that the crack distribution will be typical.

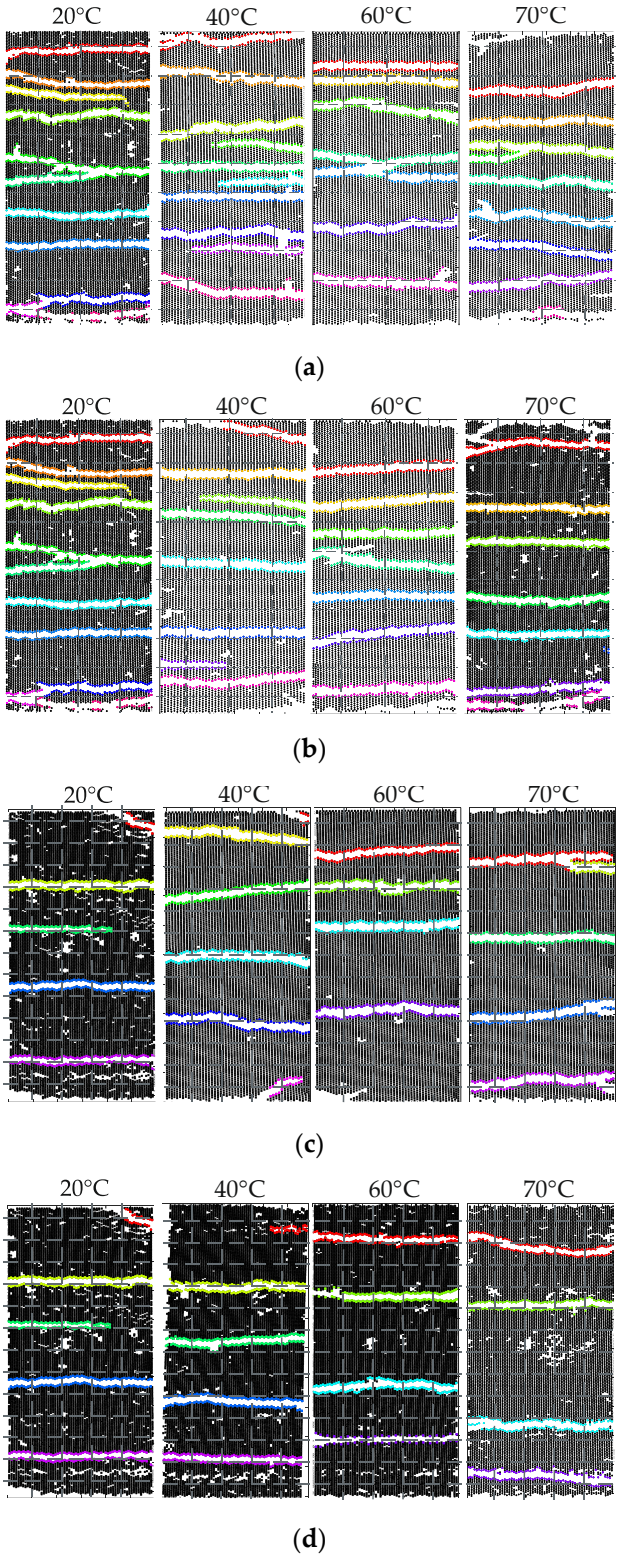

Figure 16. Exemplary crack pattern of the investigated materials immediately before failure. The textile reinforcement grid is symbolized by the dashed lines: (**a**) CTRC-EP-Sand-EH; (**b**) CTRC-EP-Sand-AH; (**c**) CTRC-P-EH; (**d**) CTRC-P-AH.

Additionally, the ratio of crack count in the failure state was analyzed to characterize crack formation. Comparing the ratio of crack count in the failure state to the available number of weft rovings in the measurement range, no discernible trend was observed with increasing temperature for the examined materials and testing methods, cf. Figure 17.

Moreover, for CTRC-EP-Sand, the ratio of crack count to weft rovings is greater, attributed to additional sanding, than for CTRC-P. Furthermore, an increase in crack numbers was noted for the tested materials with EH. This can be attributed to the discussed post-curing of the epoxy resin impregnation material.

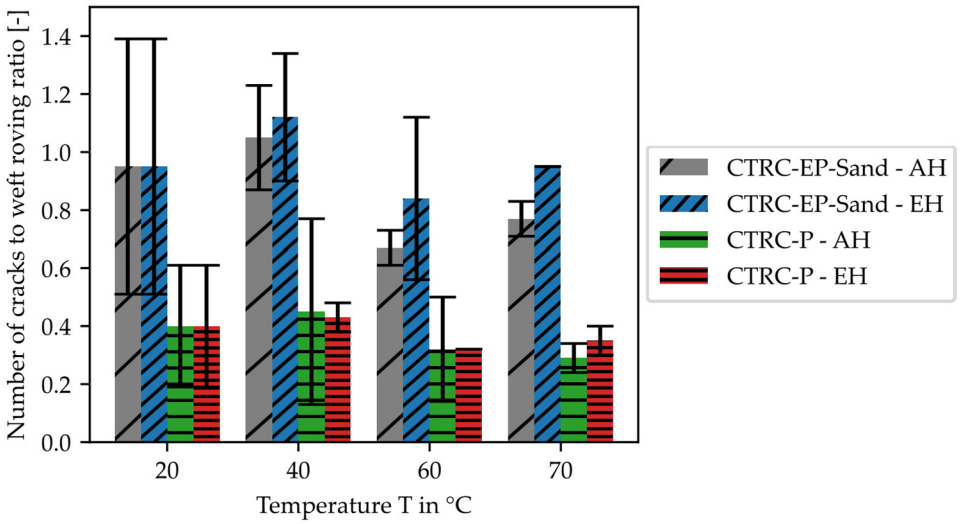

Figure 17. Ratio of the number of cracks to weft rovings in the measurement area shown as mean values with standard deviation.

5. Conclusions and Outlook

Within the framework of this investigation, the influence of electrical heating to temperatures up to 80 °C in carbon textile reinforced concrete on tensile-load-bearing behavior and crack formation of temperatures up to 80 °C were investigated. Based on the preliminary findings described, tensile strength tests on the individual components, as well as the composite, were conducted. For this purpose, two CTR, one impregnated with epoxy resin and the other with polystyrene, were connected to a laboratory power supply and electrically heated. The obtained results were compared with specimens heated in a climatic chamber and results from the literature.

The key findings of this study can be summarized as follows:

- Overall, the experimental results for electrical heating demonstrate a decrease in tensile strength in the individual components and composites of CTRC at increasing test temperatures up to 70 °C. For the fiber strand component, a decrease in tensile strength of up to 10% with EH was determined. This decline was also observed in the tensile strength results of CTRC, exhibiting a 5% reduction. In comparison with the investigated reinforcement materials, the reductions in the tensile strength of the polystyrene-impregnated CTR were lower with increasing temperature. This deviates from the results for AH.
- Upon comparing the tensile strength of CTR with that of CTRC, CTR exhibits higher tensile strength, attributed to mechanical bonding and testing effects. However, the results indicate that the electrical heating process does not induce additional effects on the composite system compared to the temperature behavior observed at elevated ambient temperatures.
- However, a crucial factor in the utilization of electrically heated CTRC is the impregnation material. The results indicate that the material properties are mainly determined by the impregnation material, particularly at elevated temperatures. Any physical and chemical changes due to temperature variations have a substantial effect on load-bearing capacity and crack formation. Moreover, the results indicate that electrical conductivity varies with different impregnation materials, highlighting the importance of selecting suitable CTR for building components.

- Moreover, the stress–strain curve for the uniaxial tensile loading of electrically heated CTRC aligns with the material characteristics known from research results in the literature.
- However, EH seems to have a positive impact on the crack distribution of epoxy resin-impregnated CTR. Based on the results of the CTRC tensile strength tests, crack distribution and crack width were analyzed. Electrical heating resulted in an elevated number of cracks while simultaneously reducing the average crack width.

These findings are crucial as they support the feasibility of integrating electrically heated CTRC into building components, providing accurate quantification of material properties through electrical heating, thereby advancing the understanding and the potential applications of this innovative material in construction. For further investigation, the impact of electrical heating on crack widths and tensile-load-bearing behavior in components subjected to freezing conditions should be characterized. For this purpose, experiments on CTRC under freezing conditions with heated CTR are planned, and the effect of heating on cracks will be further analyzed in a specific temperature range. Additionally, transient temperature tests should be conducted on the mortar within the investigated temperature range to consider creep behavior, and further analysis should focus on examining the impregnation materials, particularly the softening process. Furthermore, the experimental approach should be extended to include tests with prolonged heating periods and to investigate reversibility. Moreover, building components involving electrical heating should be manufactured and monitored.

Author Contributions: Conceptualization, methodology, software, validation, formal analysis, investigation, resources, data curation, writing—original draft preparation, visualization, A.D.; writing—review and editing, supervision, project administration, A.D. and M.R. All authors have read and agreed to the published version of the manuscript.

Funding: This research received no external funding.

Institutional Review Board Statement: Not applicable.

Informed Consent Statement: Not applicable.

Data Availability Statement: The data presented in this study are available in the article.

Conflicts of Interest: The authors declare no conflicts of interest.

References

1. Morales Cruz, C. Crack-Distributing Carbon Textile Reinforced Concrete Protection Layers. Ph.D. Thesis, RWTH Aachen University, Aachen, Germany, 2020.
2. Asgharzadeh, A. Durability of Polymer Impregnated Carbon Textiles as CP Anode for Reinforced Concrete. Ph.D. Thesis, RWTH Aachen University, Aachen, Germany, 2019.
3. Dahlhoff, A.; Morales Cruz, C.; Raupach, M. Influence of Selected Impregnation Materials on the Tensile Strength for Carbon Textile Reinforced Concrete at Elevated Temperatures. *Buildings* **2022**, *12*, 2177. [CrossRef]
4. Tröger, M.S.F.; Große, M.S.S.; Rudloff, M.E.D.-I.T.; Heimbold, I.T. Entwicklung einer elektrischen Kontaktierung für multifunktionale Carbonfaser-Strukturen in Beton. In Proceedings of the 19th AALE-Konferenz, Luxemburg, 8–10 March 2023.
5. Hasan, M.; Offermann, M.; Haupt, M.; Nocke, A.; Cherif, C. Carbon filament yarn-based hybrid yarn for the heating of textile-reinforced concrete. *J. Ind. Text.* **2014**, *44*, 183–197. [CrossRef]
6. Gerlach, F.; Ahlborn, K.; Vonau, W.; Wolf, B.; Hoffmann, K. Applikation textiler Flächenelektroden zur Zustandsüberwachung und Sanierung von Baukörpern. In Proceedings of the 18th GMA/ITG-Fachtagung Sensoren und Messsysteme 2016, Nürnberg, Germany, 10–11 May 2016; pp. 493–499.
7. Schladitz, F.; Lägel, E.; Ehlig, D.; Nietner, L.; Tietze, M. Carbon reinforced concrete and temperature. In Proceedings of the IABSE Congress—The Evolving Metropolis, New York City, NY, USA, 4–6 September 2019; pp. 486–492.
8. Hemmen, A. Direktbestromung von Kohlenstofffasern zur Minimierung von Zykluszeit und Energieaufwand bei der Herstellung von Karbonbauteilen. Ph.D. Thesis, Universität Augsburg, Augsburg, Germany, 2016.
9. Krois, K. Entwicklung Eines Elektrischen Energiespeichers zur Integration in Carbonbeton. Ph.D. Thesis, Technische Universität Darmstadt, Darmstadt, Germany, 2021.
10. Dahlhoff, A.; Raupach, M. Elektrisch beheizbarer textilbewehrter Carbonbeton. In Proceedings of the 21th Ibausil—Internationale Baustofftagung Weimar, Weimar, Germany, 13–15 September 2023.

11. Schöffel, J.; Abdelkaf, N. Rethinking construction: The market for heatable carbon concrete building components. In *Fraunhofer-Zentrum für Internationales Management und Wissensökonomie IMW Jahresbericht 2018/2019*; Fraunhofer Center for International Management and Knowledge Economy IMW: Leipzig, Germany, 2019; pp. 66–67.
12. C³InteF—Integration der Heizfunktion in Bauelementen aus Carbonbeton. Available online: https://www.imw.fraunhofer.de/de/forschung/unternehmensentwicklung/geschaeftsmodelle/projekte/c-intef.html (accessed on 25 February 2024).
13. Load-Bearing Concrete Members with Adaptive Heating Structures Made of Carbon Fibres for Buildings with Climate Neutral Energy Strategy. Available online: https://tu-dresden.de/bu/bauingenieurwesen/imb/forschung/Forschungsfelder/CRC/fue-crc/FuE_finished/smarttex?set_language=en (accessed on 25 February 2024).
14. Frenzel, M.; Stelzmann, M.; Söhnchen, A. CUBE—Demonstration areas and exhibition objects. *Beton-Und Stahlbetonbau* **2023**, *118*, 133–139. [CrossRef]
15. Abdualla, H.; Ceylan, H.; Kim, S.; Gopalakrishnan, K.; Taylor, P.C.; Turkan, Y. System requirements for electrically conductive concrete heated pavements. *Transp. Res. Rec.* **2016**, *2569*, 70–79. [CrossRef]
16. Liu, Y.; Lai, Y.; Ma, D. Melting snow on airport cement concrete pavement with carbon fibre heating wires. *Mater. Res. Innov.* **2015**, *19*, S10–S95. [CrossRef]
17. Xu, S.; Yu, W.; Song, S. Numerical simulation and experimental study on electrothermal properties of carbon/glass fiber hybrid textile reinforced concrete. *Sci. China Technol. Sci.* **2011**, *54*, 2421–2428. [CrossRef]
18. Kapsalis, P.; Tysmans, T.; Van Hemelrijck, D.; Triantafillou, T. State-of-the-Art Review on Experimental Investigations of Textile-Reinforced Concrete Exposed to High Temperatures. *J. Compos. Sci.* **2021**, *5*, 290. [CrossRef]
19. Donnini, J.; De Caso y Basalo, F.; Corinaldesi, V.; Lancioni, G.; Nanni, A. Fabric-reinforced cementitious matrix behavior at high-temperature: Experimental and numerical results. *Compos. Part B Eng.* **2017**, *108*, 108–121. [CrossRef]
20. Rambo, D.A.S.; Yao, Y.; de Andrade Silva, F.; Toledo Filho, R.D.; Mobasher, B. Experimental investigation and modelling of the temperature effects on the tensile behavior of textile reinforced refractory concretes. *Cem. Concr. Compos.* **2017**, *75*, 51–61. [CrossRef]
21. Rambo, D.A.S.; de Andrade Silva, F.; Toledo Filho, R.D.; da Fonseca Martins Gomes, O. Effect of elevated temperatures on the mechanical behavior of basalt textile reinforced refractory concrete. *Mater. Des. (1980–2015)* **2015**, *65*, 24–33. [CrossRef]
22. Lenting, M. Untersuchungen zu Mineralischen Tränkungen von Technischen Textilien für die Flächige Instandsetzung von Gerissenen Bauwerken Mit Textilbeton. Ph.D. Thesis, Technische Universität Dortmund, Dortmund, Germany, 2023.
23. Rambo, D.; Silva, F.; Toledo Filho, R.; Ukrainczyk, N.; Koenders, E. Tensile strength of a calcium-aluminate cementitious composite reinforced with basalt textile in a high-temperature environment. *Cem. Concr. Compos.* **2016**, *70*, 183–193. [CrossRef]
24. TR IH. *Technische Regel—Instandhaltung von Betonbauwerken (TR Instandhaltung)—Teil 1: Anwendungsbereich und Planung der Instandhaltung*; Deutsches Institut für Bautechnik (DIBt): Berlin, Germany, 2020.
25. TR IH. *Technische Regel—Instandhaltung von Betonbauwerken (TR Instandhaltung)—Teil 2: Merkmale von Produkten oder Systemen für die Instand-Setzung und Regelungen für Deren Verwendung*; Deutsches Institut für Bautechnik (DIBt): Berlin, Germany, 2020.
26. Technical Product Data Sheet—Solidian. Available online: https://solidian.com/downloads/ (accessed on 12 October 2023).
27. *ASTM C307-18*; Standard Test Method for Tensile Strength of Chemical-Resistant Mortar, Grouts, and Monolithic Surfacings. American Society of Testing and Materials: West Conshohocken, PA, USA, 2018.
28. Dahlhoff, A.; Winkels, B.; Morales Cruz, C.; Raupach, M. Investigations on the Experimental Setup for Testing the Centric Tensile Strength According to ASTM C307 of Mineral-based Materials. *J. Civ. Eng. Constr.* **2022**, *11*, 239–254. [CrossRef]
29. *DIN EN 1015-3*; Methods of Test for Mortar for Masonry—Part 3: Determination of Consistence of Fresh Mortar (by Flow Table); German Version EN 1015-3:1999+A1:2004+A2:2006. iTeh, Inc.: Newark, DE, USA, 2007.
30. *DIN EN 1015-6*; Methods of Test for Mortar for Masonry—Part 6: Determination of Bulk Density of Fresh Mortar; German Version EN 1015-6:1998+A1:2006. iTeh, Inc.: Newark, DE, USA, 2007.
31. *DIN EN 1015-7*; Methods of Test for Mortar for Masonry—Part 7: Determination of Air Content of Fresh Mortar; German Version EN 1015-7:1998. iTeh, Inc.: Newark, DE, USA, 1998.
32. *DIN EN 1015-11*; Prüfverfahren für Mörtel für Mauerwerk—Teil 11: Bestimmung der Biegezug- und Druckfestigkeit von Festmörtel; Deutsche Fassung EN 1015-11:2019. Beuth Verlag GmbH: Berlin, Germany, 2020.
33. Schütze, E.; Bielak, J.; Scheerer, S.; Hegger, J.; Curbach, M. Uniaxial tensile test for carbon reinforced concrete with textile reinforcement. *Beton-Und Stahlbetonbau* **2018**, *113*, 33–47. [CrossRef]
34. Dahlhoff, A.; Raupach, M. Crack Analysis of Textile Reinforced Concrete Using Automated Crack Evaluation via Digital Image Correlation. *Buildings* **2023**, *13*, 2984. [CrossRef]
35. Rieger, J. The glass transition temperature of polystyrene: Results of a round robin test. *J. Therm. Anal. Calorim.* **1996**, *46*, 965–972. [CrossRef]
36. Baur, E.; Drummer, D.; Osswald, T.A.; Rudolph, N. *Saechtling Kunststoff-Handbuch: Eigenschaften, Verarbeitung, Konstruktion*; Carl Hanser Verlag GmbH Co KG: Munich, Germany, 2022.
37. Schneider, U. *Behaviour of Concrete at High Temperatures—Deutscher Ausschuss für Stahlbeton e. V.*; Erst & Sohn: Berlin, Germany; München, Germany, 1982.
38. Holz, K. Carbon Reinforced Concrete Exposed to High Temperature. Ph.D. Thesis, Technische Universität Dresden, Dresden, Germany, 2021.

39. Kulas, C.; Hegger, J.; Raupach, M.; Antons, U. Experimental and theoretical investigations on the high-temperature behavior of fine-grained concrete and textile yarns. *Beton-Und Stahlbetonbau* **2011**, *106*, 707–715. [CrossRef]
40. Rempel, S. Reliability of the Structural Design for Concrete Elements with Textile Reinforcement and Bending Load. Ph.D. Thesis, Rheinisch-Westfälische Technische Hochschule Aachen University, Aachen, Germany, 2018.
41. Kalthoff, M. Extruded Thin-Walled Textile Reinforced Concrete Components with Flexible Shape. Ph.D. Thesis, RWTH Aachen University, Aachen, Germany, 2023.
42. Jesse, F. Bearing Behavior of Filament Yarns in a Cementitious Matrix. Ph.D. Thesis, Technische Universität Dresden, Dresden, Germany, 2005.
43. Hansl, M.; Feix, J. Investigation of crack width in textile reinforced concrete. *Beton-Und Stahlbetonbau* **2015**, *110*, 410–418. [CrossRef]
44. Niederwald, M. Zum Einfluss der Viskoelastischen Eigenschaften des Beschichteten Bewehrungsmaterials auf das Zugtragverhalten von Carbonbewehrtem Beton. Ph.D. Thesis, Universität der Bundeswehr München, München, Germany, 2017.